

Multi-Alternating Organic Semiconducting Films with High Electric Conductivity

Hin-Wai Mo, Ming-Fai Lo, Qing-Dan Yang, Tsz-Wai Ng,* and Chun-Sing Lee*

High electric conductivity is observed in multilayer stack of m-MTDATA/ F_{16} CuPc. Impedance data shows that the circuit resistance is significantly dropped by three orders of magnitude from ~ 0.2 M Ω to ~ 0.4 k Ω when the number of alternating units is increased from one to six, keeping a total thickness of 300 nm. Impedance results show that as the number of alternating units increases, the organic stack shows an increasing capacitance and a decreasing resistance. This result suggests the increasing charges accumulate at the heterojunctions, leading to reduction in overall film resistance. The application of the high conductive units in OLED device results in stability enhancement.

Recent studies reported that device incorporating multi-alternating films exhibit properties that are significantly different from those of bulk and planar heterojunctions.^[14] For example, Yokoyama et al. showed a change of up to 0.58 in refractive index by using a multilayer stack.^[15] In this work, we demonstrated that a multi-alternating 4,4',4''-Tris(N-3-methylphenyl-N-phenylamino) triphenylamine (m-MTDATA)/ F_{16} CuPc stack exhibits ohmic conductivity which is observed neither in the corresponding bilayer nor bulk heterojunction.

1. Introduction

Intrinsic organic semiconducting films show poor electric conductivities^[1] due to their low charge carrier densities and charge hopping transport.^[2] However, recent studies have shown that some organic-organic and inorganic-organic pairs with strong charge interaction show much higher conductivities along their interfaces.^[3–8] For example, Alves et al. showed that the contact of two single crystals (i.e. tetrathiofulvalene TTF/7,7,8,8-tetracyanoquinodimethane TCNQ) form a metallic conducting interfaces^[3] with conductivity exceeding 10^5 S/cm.^[9,10] Qiao et al. also reported similar increment in current density by at least two orders of magnitude when MoO_3 is doped in hole-transporting organic semiconducting film.^[11] While most studies attributed the observed high conductivity to charge exchange process between the two components, it is later noted that the conductivity depends strongly on the devices configuration. Wang et al. showed that the bilayer structured copper phthalocyanine (CuPc)/copper hexadecafluorophthalocyanine (F_{16} CuPc) show high conductivity. However the conductivity of a mixed sample (i.e. CuPc: F_{16} CuPc; mixing ratio of 1:1) is only similar to those of the individual semiconducting film.^[12,13]

2. Results and Discussion

Figure 1 shows the current density-voltage (J - V) characteristics of two devices with respectively 1 (dashed line) and 30 (solid line) units of “m-MTDATA/ F_{16} CuPc” bilayers (same total thickness of 300 nm) in the configuration of ITO/1 or 30 units of bilayer (300 nm)/BPhen (8 nm)/Al. At a bias of 1.5 V, the current density in the 30-units device is 267 mA/cm² which is about 3 orders of magnitude higher than that in the 1-unit device.

One possible explanation to the high current density observed in Figure 1 is instant electrical shorting upon deposition of Al electrodes on the multi-layer organic films. Multi-layer films with high roughness might results in electrical shorting if the two electrodes are too close to each other. We therefore examined the surface morphologies of 1, 7 and 30 units of bilayer films with overall thickness kept at 300 nm using atomic force microscope (AFM). Figure S1 compares the AFM image of the multi-layered films. The root-mean-square surface roughness (R_{rms}) of 1, 7 and 30 units of bilayer films are 0.464 nm, 0.863 nm and 1.417 nm, respectively. These measured roughnesses are two order-of-magnitudes smaller than the individual thickness of each organic stack. These results suggest that the conductivity differences in Figure 1 cannot be explained by the possible roughness differences.

Another possible explanation is that the metal atoms diffuse into the multilayer stack with porous structure, which leads to low resistance links between the two electrodes. To rule out this possibility, we prepared organic light-emitting devices (OLEDs) on ITO substrate with or without a stack of [m-MTDATA (5 nm)/ F_{16} CuPc (5 nm)] \times 7. The device configuration is: ITO/7-unit of bilayer (70 or 0 nm)/NPB (70 nm)/Alq₃ (60 nm)/LiF (1 nm)/Al. Figure 2a shows that even with an extra 70 nm

H.-W. Mo, Dr. M.-F. Lo, Dr. Q.-D. Yang, Dr. T.-W. Ng, Prof. C.-S. Lee

Department of Physics and Materials Science
Center of Super-Diamond
and Advanced Films (COSDAF)

City University of Hong Kong
Hong Kong SAR, Hong Kong

E-mail: tszwaing@cityu.edu.hk; apcslee@cityu.edu.hk

Dr. M.-F. Lo, Dr. T.-W. Ng, Prof. C.-S. Lee
City University of Hong Kong Shenzhen Research Institute
Shenzhen, PR China



DOI: 10.1002/adfm.201400468

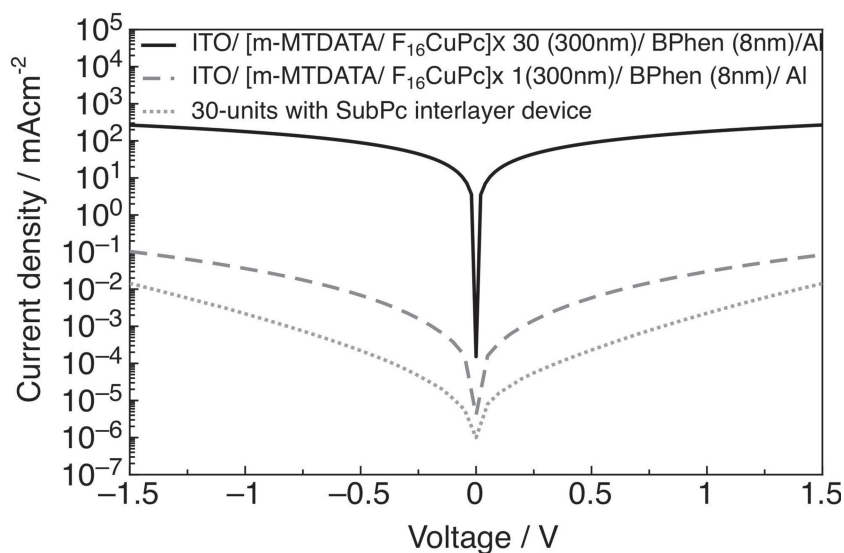


Figure 1. J–V characteristic of the 30-unit device (solid-line), single unit devices (dashed-line) and 30-units with SubPc interlayer device (dotted-line). The device configuration: ITO/[m-MTDATA/F₁₆CuPc] × 30 (300 nm)/BPhen (8 nm)/Al, ITO/m-MTDATA (150 nm)/F₁₆CuPc (150 nm)/BPhen (8 nm)/Al, and ITO/[m-MTDATA (4 nm)/SubPc (1 nm)/F₁₆CuPc (4 nm)/SubPc (1 nm)] × 29/m-MTDATA (4 nm)/SubPc (1 nm)/F₁₆CuPc (4 nm)/BPhen (8 nm)/Al.

stack of multilayer, the device shows negligible difference in the current density–luminance–voltage characteristics with those of the control device. These suggest that (1) the multilayer stack add negligible serial resistance to the device and (2) its high conductivity cannot be explained by the cathode diffusion. In fact the extra multilayer stack does endow the device with better operation stability as shown in Figure 2b. This can be explained by an extra diffusion barrier to protect the emitting unit from the harmful oxygen species from the ITO substrate.^[16]

We also measured the resistivity of the 30-unit device at temperatures of 173–293 K and the results are shown in Figure S2. Resistivity of the device increases as the temperature decreases. This shows that the multilayer stack has semiconductor characteristics. To further explore the mechanisms of the high conductivity of the multilayer stack, we carried out a control experiment in which, a 1 nm thick SubPc layer is inserted at each interface of the m-MTDATA/F₁₆CuPc bilayers in the 30-unit device (thickness of each m-MTDATA and F₁₆CuPc layer is reduced from 5 to 4 nm to keep the total thickness constant). It is interesting that the conductivity of the control device (dotted line in Figure 1) is about four orders lower than the original 30-unit device (solid line). In fact the conductivity of the control device is even lower than that of the 1-unit device (dashed line). This suggests that the high conductivity of the original 30-unit stack is related to the m-MTDATA/F₁₆CuPc interface.

To further understand the effect of heterojunction in the conductivity, the different numbers of alternating unit are studied. Keeping the overall thickness of m-MTDATA/F₁₆CuPc stacks at 300 nm, the devices with structure of ITO/[m-MTDATA/F₁₆CuPc] × *n* (300 nm)/BPhen (8 nm)/Al devices where *n* = 1 (single-unit device), 3 (3-unit device), 6 (6-unit device) and 30 (30-unit device) are fabricated. Their impedance responses at various applied voltage are measured.^[17–20]

Figure 3a shows the impedance spectra of the devices in complex plane at an applied bias of 3V. The measured data are shown as symbols. A semi-circle in the complex plane is observed where the Y-axis representing an imaginary part of impedance response (*Z''*) and the X-axis refer to the real part of the impedance response (*Z'*). The measured data is modeled (lines in Figure 3a) by an equivalent circuit diagram as shown in Figure 3b. *R_s*, representing the resistance from the organic/electrode interfaces,^[20] of the circuit can be determined from the x-intercepts of the semicircles at the high frequency end. It can be seen from Figure 3a that *R_s* for all the devices with different numbers of m-MTDATA/F₁₆CuPc bilayers are about 40 Ohm, suggesting that they have similar resistances at the organic/electrode interfaces.^[20] This can be well understood as all these devices have the same organic/electrode interfaces.

Diameter of the semi-circle, reflecting the *R₁*, decreases with increasing the number of alternating unit (*n*).^[17] For *n* = 1, 3, 6 and

30, the capacitance, *C₁*, are determined to be 2.6, 4.4, 21 and 350 nF, respectively. Both the increase in *C₁* and the decrease in *R₁* observed when increasing number of alternating unit *n* suggest the increased accumulated charges at the heterojunctions leading to reduction in overall device resistance.^[21] The calculated conductivity of the 30-unit device at zero applied bias has value of 4×10^2 S/cm. This value is considerably lower than the extremely high conductivity of 10^5 S/cm along the interface between TTF/TCNQ single crystals which form charge transfer complex (CTC).^[9,10] This difference can be attributed to the amorphous nature in the present films. On the other hand, it should be noted that in the single crystal experiment, the conductivity is measured along the interface where the two single crystal form CTC. In the present experiment, the conductivity is measured perpendicular to the CTC interface and this is expected to give a lower conductivity than along the interface.

Figure 3c shows the impedance spectrum of 30 units with SubPc interlayer device which has a much larger diameter compared to other devices without the SubPc interlayer (Figure 3a). It can be seen that this device has a much higher resistance and an estimated conductivity of 2×10^{-3} S/cm.

It is also noted in Figure 3c, the line cannot satisfactorily modeled with a simple circuit shown in Figure 3b. The discrepancy is mainly caused by the deviation from the semicircle shape at the high frequency end (see inset of Figure 3c for a magnified view). To satisfactorily fit the impedance curve, a more complicated circuit involving a constant phase element (CPE) in parallel with a resistor *R₁* as shown in Figure 3d is needed. The CPE has an impedance of $Z = Q(j\omega)^\phi$ and a capacitance $C = (R_1 Q)^{1/\phi} / R_1$, where ϕ represents an “ideality” factor characteristics of the CPE, with $\phi = 1$ corresponds to an ideal capacitor and ϕ in this study is about 0.81, and *Q* is the magnitude, with further details reported elsewhere.^[22]

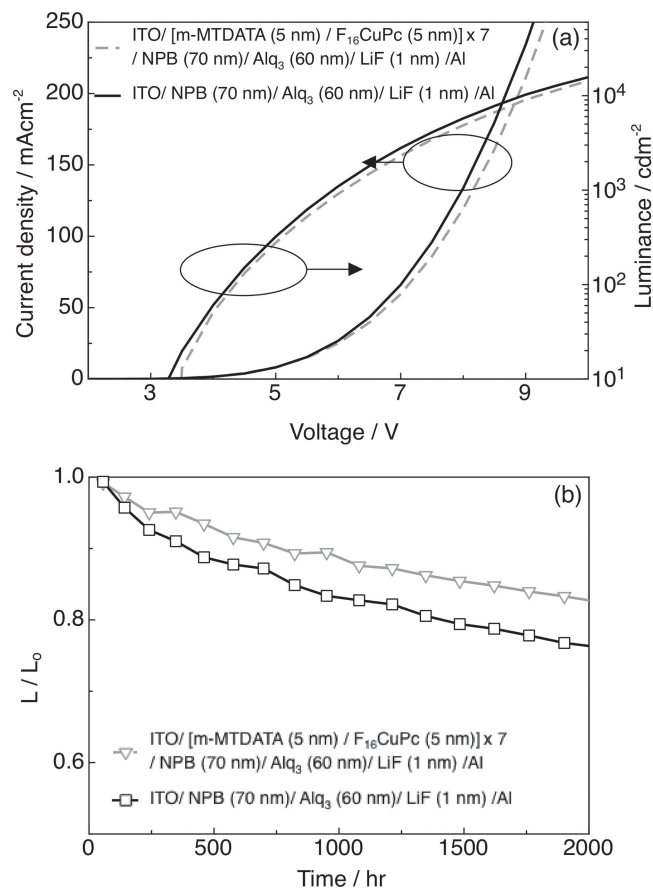


Figure 2. (a) J–V–L characteristics of the OLED devices with and without the multi-alternating unit. Device configuration: ITO/[m-MTDATA (5 nm)/F₁₆CuPc (5 nm)] × 0 or 7/NPB (70 nm)/Alq₃ (60 nm)/LiF (1 nm)/Al. (b) Luminance of the OLED with and without the multi-alternating unit as a function of time.

The resistance, R_1 , of these devices were calculated from the impedance spectrum and plotted in **Figure 4**. Device with $n = 30$ shows an ohmic conduction with resistance remains in range of $10^1 \Omega$ over the applied bias from 0 to 3 V. Devices with $n = 1$ and $n = 3$ clearly show a decrease in resistance when the applied bias increased. This suggests a rectifying property that commonly observed in semiconducting film.

In contrast to the high conductivity observed along the interface as reported in literatures, our finding here presented a high conductivity even for a thick multi-layer stack (300 nm) with charge flow direction perpendicular to the contact interface. Detail mechanisms for such conductivity enhancement perpendicular to the donor–acceptor interface are not fully understood. Nevertheless, one possible mechanism is due to the substantial increase in mobile charge density upon forming the multilayer stack. Our previous surface electronic studies^[24] show a surface dipole formation at the contact interface of m-MTDATA/F₁₆CuPc with considerable interfacial surface states generation such that their energy levels are energetically pinned at the Fermi levels as shown in **Figure 5a**.^[23,24] These abrupt energy level shift results in a small offset of 0.4 eV between the HOMO of m-MTDATA and the LUMO of F₁₆CuPc which facilitates effective charge transfer at the m-MTDATA/F₁₆CuPc interface. The 1-unit bilayer device consists of only a single m-MTDATA/F₁₆CuPc interface such that the observed current flow in the device (dashed line in Figure 1a) is dominated by charge hopping transport in the thick layer m-MTDATA and F₁₆CuPc semiconducting films. In the multiplayer stack, the spacing between the dipole decreases as the number of layer increases. This results in a high density of interfaces with a large amount of mobile interfacial charges thoroughly distributed along the 300 nm stack (**Figure 5b**).^[25,26] This observation is consistent with the high capacitance of the 30-unit device. The surface generated electronic states, together with the interfacial built-in E-field at the contacts, contribute to the charge carrier transport

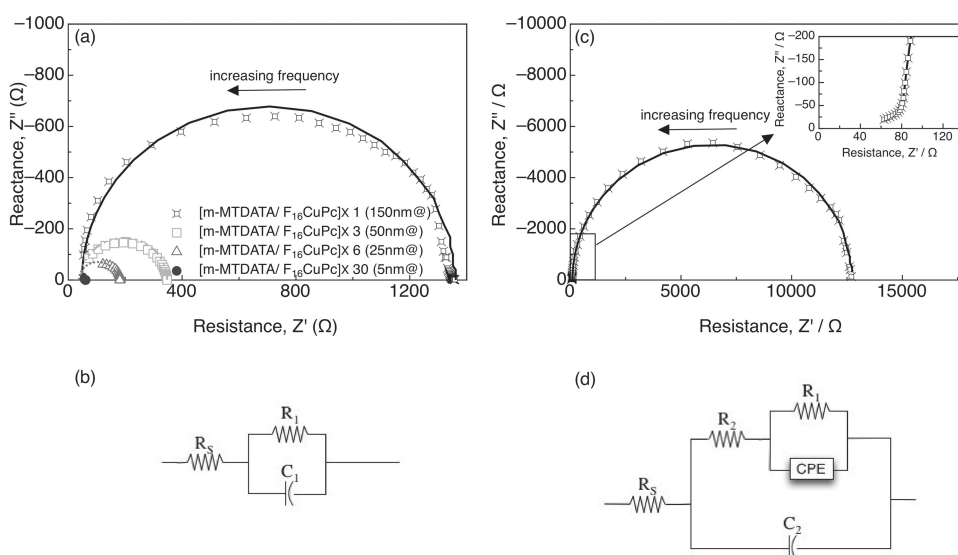


Figure 3. (a) Impedance response of number of multi-alternating unit $n = 1, 3, 6$ and 30 that measured at applied bias of $3V$. (b) Equivalent circuit of the devices listed in (a). (c) Impedance response of 30 -units with SubPc interlayer device. (d) Equivalent circuit of the device listed in (c).

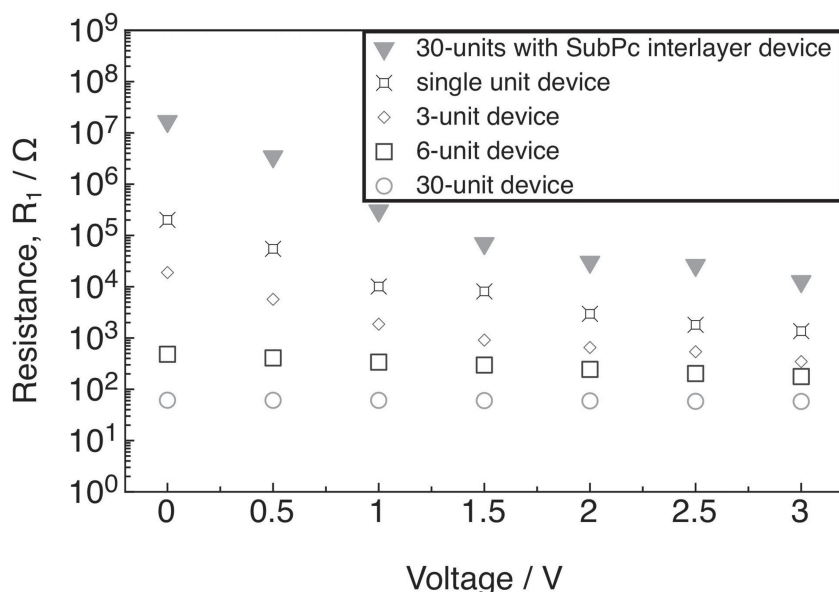


Figure 4. Plot of resistance, R_1 extracted from impedance spectra as a function of applied bias

by promoting charge exchange process between the LUMO of $F_{16}CuPc$ and the HOMO of the m-MTDATA.

3. Conclusion

We show that multi-alternating m-MTDATA/ $F_{16}CuPc$ films have high conductivity up to $S = 4 \times 10^2$ S/cm. Impedance spectroscopic studies show that the conductivity of the multi-alternating m-MTDATA/ $F_{16}CuPc$ films depends strongly on the individual film thickness and the number of alternating units. The increase in the number of alternating units (n) results respectively in an increase in capacitance and a decrease in resistance of the stack. This result suggests the increasing charges accumulated at the heterojunctions leading to reduction in overall device resistance. When this

multi-alternating unit applied near the ITO anode of the OLED, stability enhancement with negligible change in turn-on voltage and EL emission is observed.

4. Experimental Section

Device Fabrication and J–V Characteristics: Devices were fabricated on $30 \Omega/\text{square}$ patterned indium-tin oxide (ITO) coated glass substrates, which were cleaned with Decon 90, and rinsed in de-ionized water and dried in an oven. The substrates were UV ozone treated before loading into a vacuum deposition chamber. All organic films were thermally evaporated under 10^{-7} Torr with deposition rates controlled between 1 to 2 Å/s. Active areas of the devices were defined by the overlapping region of the ITO cathode and the Al anode which is 0.1 cm^2 . All devices were then encapsulated under a nitrogen environment. In order to have better comparison of the J–V characteristics, the total thickness of organic layers is 300 nm in all devices. Current density–voltage (J–V) characteristics were measured with a programmable Keithley model 237 power source in dark. For resistivity measurement, device

was kept in a DELTA 9023 environmental chamber to obtain different temperatures.

Impedance Spectroscopy: Impedances of the devices were measured with a Zahner IM 6 electrochemical workstation over 10 mHz to 1 MHz with an oscillation amplitude of 50 mV. Conductivity is calculated from the resistance value extracted from impedance response using the equation of $\sigma = 1/Rt$, where σ is the conductivity, R is the resistance extracted from the equivalent circuit and t is the thickness of the organic layers.

OLED Characterization: Current density–voltage–luminance (J–V–L) characteristics, CIE coordinates, and electroluminescent (EL) spectra were measured with a Photoresearch PR650 photometer.

Supporting Information

Supporting Information is available from the Wiley Online Library or from the author.

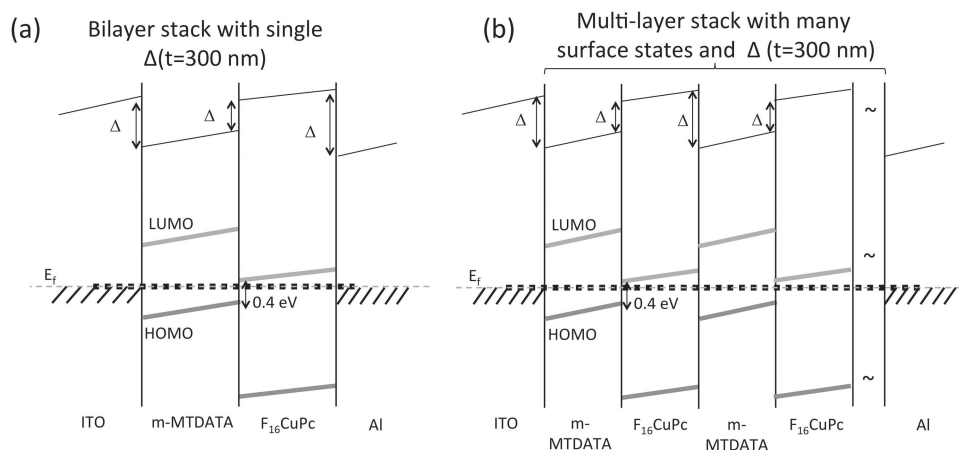


Figure 5. Energy level diagrams of a (a) bilayer and a (b) multi-layered m-MTDATA/ $F_{16}CuPc$ interface.

Acknowledgements

The work described in this paper was supported by a grant from the Research Grants Council of the Hong Kong Special Administrative Region, China (Project No. T23-713/11); and National Natural Science Foundation of China (No. 21303150). We also thank Prof C.W. Tang for useful discussion.

Received: February 10, 2014

Revised: April 3, 2014

Published online: June 23, 2014

-
- [1] H. Nakanotani, H. Kakizoe, C. Adachi, *Solid State Commun.* **2010**, 151, 93.
- [2] S. J. Yoo, J. H. Lee, J. H. Lee, J. J. Kim, *Appl. Phys. Lett.* **2013**, 102, 193301.
- [3] H. Alves, A. S. Molinari, H. Xie, A. F. Morpurgo, *Nat. Mater.* **2008**, 7, 574.
- [4] J. R. Kirtley, J. Mannhart, *Nat. Mater.* **2008**, 7, 520.
- [5] M. Nakano, H. Alves, A. S. Molinari, S. Ono, N. Minder, A. F. Morpurgo, *Appl. Phys. Lett.* **2010**, 96, 232102.
- [6] S. Wen, W. Q. Deng, K. L. Han, *Chem. Commun.* **2010**, 46, 5133.
- [7] H. Nakanotani, H. Kakizoe, C. Adachi, *Solid State Commun.* **2011**, 151, 93.
- [8] Y. Kitamura, E. Shikoh, K. Sawabe, T. Takenobu, M. Shiraishi, *Appl. Phys. Lett.* **2012**, 101, 073501.
- [9] J. Ferraris, D. O. Cowan, V. Walatka, Jr., J. H. Perlstein, *J. Am. Chem. Soc.* **1973**, 95, 948.
- [10] Denis Jerome, *Chem. Rev.* **2004**, 104, 5565.
- [11] X. F. Qiao, J. S. Chen, X. L. Li, D. G. Ma, *J. Appl. Phys.* **2010**, 107, 104505.
- [12] J. Wang, H. B. Wang, X. J. Yan, H. C. Huang, D. H. Yan, *Appl. Phys. Lett.* **2005**, 87, 093507.
- [13] F. Zhu, H. B. Wang, D. Song, K. Lou, D. H. Yan, *Appl. Phys. Lett.* **2008**, 93, 103308.
- [14] P. J. Jadhav, A. Mohanty, J. Sussman, J. Lee, M. A. Baldo, *Nano Lett.* **2011**, 11, 1495.
- [15] D. Yokoyama, K.-i. Nakayama, T. Otani, J. Kido, *Adv. Mater.* **2012**, 24, 6368.
- [16] M. F. Lo, T. W. Ng, H. W. Mo, C. S. Lee, *Adv. Funct. Mater.* **2013**, 23, 1718.
- [17] B. J. Leever, C. A. Bailey, T. J. Marks, M. C. Hersam, M. F. Durstock, *Adv. Energy Mater.* **2012**, 2, 120.
- [18] L. Burtone, D. Ray, K. Leo, M. Riede, *Appl. Phys. Lett.* **2012**, 111, 064503.
- [19] G. Garcia-Belmonte, A. Munar, E. M. Barea, J. Bisquert, I. Ugarte, R. Pacios, *Org. Electron.* **2008**, 9, 847.
- [20] G. G. Belmonte, P. P. Boix, J. Bisquert, M. Sessolo, H. J. Bolink, *Solar Energy Mater. Solar Cells* **2010**, 94, 366.
- [21] K. Kawano, C. Adachi, *Adv. Funct. Mater.* **2009**, 19, 3934.
- [22] J. R. Macdonald, *Impedance Spectroscopy*, John Wiley & Sons, NJ, USA **1987**.
- [23] S. Braun, X. Liu, W. R. Salaneck, M. Fahlman, *Org. Electron.* **2010**, 11, 212.
- [24] H. W. Mo, T. W. Ng, C. H. To, M. F. Lo, J. A. Zapien, C. S. Lee, *Org. Electron.* **2013**, 14, 291.
- [25] H. Wang, Z. Liu, M. F. Lo, T. W. Ng, D. Yan, C. S. Lee, *Appl. Phys. Lett.* **2012**, 100, 103302.
- [26] K. M. Lau, J. X. Tang, H. Y. Sun, C. S. Lee, S. T. Lee, D. H. Yan, *Appl. Phys. Lett.* **2006**, 88, 173513.
-